Journal of Computational and Applied Mathematics 438 (2024) 115540

Contents lists available at ScienceDirect

Journal of Computational and Applied Mathematics

journal homepage: www.elsevier.com/locate/cam

Improved enrichments and numerical integrations in SGFEM for interface problems

Wenbo Gong [a], Hengguang Li [b,1], Qinghui Zhang [a,c,*,2]

[a] School of Science, Harbin Institute of Technology, Shenzhen, 518000, PR China
[b] Department of Mathematics, Wayne State University, Detroit, MI 48202, USA
[c] Guangdong Province Key Laboratory of Computational Science, Guangzhou, 510006, PR China

ARTICLE INFO

Article history:
Received 30 December 2021
Received in revised form 20 August 2023

Keywords:
GFEM/XFEM
SGFEM
Interface
Enrichment
Numerical integration

ABSTRACT

Generalized/extended finite element methods (GFEM/XFEM) for an interface problem are generally enriched by a distance function to the interface to handle discontinuities across the interface. Evaluations of the distance function and its gradients are needed for assembling stiffness matrices, which requires certain computational geometry algorithms. The computational complexity grows if the number of integration points is increased. Besides, the mathematical analysis on the effect of numerical integration has not been established in the field of GFEM/XFEM yet. This study designs an improved enriched function for a stable GFEM (SGFEM, a stable version of GFEM) based on the distance function, which only requires evaluating the distance function at nodes of elements that interact the interface (the gradients of distance function are not needed). The optimal convergence order (in the energy norm) of the SGFEM with such an improved enriched function is proven. In turn, we propose a perturbed variational formula, which can be integrated exactly by simple Gaussian rules designed in this paper. We prove that the SGFEM based on the improved enriched function and the perturbed variational formula (exactly integrated by the numerical integration) achieves the optimal convergence order for the interface problem. Namely, we develop a numerical integration rule for the SGFEM such that the optimal convergence order of SGFEM is maintained for the interface problem. The theoretical achievements are verified by numerical experiments.

1. Introduction

Interface problems exist in numerous engineering applications and multi-physical phenomena, such as fluid–structure interaction, bimaterials, multiphase flows, flows in porous media, three dimensional fiber composites [1–3]. Solutions of interface problems are generally non-smooth, which may involve jumps, kinks, singularities, and oscillations [4]. Conventional finite element methods (FEM) have to require a mesh to *fit* the interface (mesh matching or mesh refinement) to avoid loss of accuracy [5–7]. However, creating a mesh fitting the interface can be extremely difficult, especially in three-dimensional time-dependent problems. In the recent years, *unfitted* FEMs for the interface problem

* Corresponding author at: School of Science, Harbin Institute of Technology, Shenzhen, 518000, PR China.
E-mail addresses: gongwenbo@hit.edu.cn (W. Gong), li@wayne.edu (H. Li), zhangqh@hit.edu.cn, zhangqh6@mail.sysu.edu.cn (Q. Zhang).

1 This research was partially supported by the NSF Grant DMS-1819041 and the Wayne State University Career Development Chair Award.

2 This research was partially supported by the Natural Science Foundation of China under grant 11471343 and Guangdong Provincial Natural Science Foundation of China under grant 2022A1515011187.

https://doi.org/10.1016/j.cam.2023.115540
0377-0427/

have made significant progress. A FEM is called unfitted if it uses a mesh that is simple, fixed, and independent of the interface.

Typical unfitted FEMs for the interface problem include immersed FEM, penalty FEM, generalized or extended FEM (GFEM/XFEM). The immersed FEM modifies the standard FEM shape functions based on interface conditions and material coefficients [8]. This makes the construction of shape functions complex when underlying equations involve complex constitutive relationships (between strain and stress), such as vector-valued equations (elasticity systems) [9,10], anisotropic materials, and nonlinear equations. The penalty methods, e.g., cut FEM, interface penalized FEM, discontinuous Galerkin method (DGM) [11–17], use discontinuous shape functions even for the interface problem where the solution is continuous. Such a discontinuity causes a nonconforming feature in the variational problem, which is generally handled by penalty terms and parameters. The determination of the penalty parameters, however, is technical and cannot be treated using a unified approach. We mention that the shape functions of immersed FEM are also discontinuous in two- and three-dimensional problems, and the penalty technique is needed [18] consequently. This study is mainly focused on the GFEM/XFEM. The shape functions of GFEM/XFEM are constructed only based on interface geometries, and thus they are independent of the constitutive relationship and material coefficients. In addition, it is easy for the GFEM/XFEM to construct the continuous shape functions so that the conforming variational formulations can be employed without any penalty terms and parameters.

The idea of GFEM/XFEM is to *augment* the standard FEM (unfitted mesh) with special functions that mimic local features of exact solutions to solve complicated non-smooth problems [4,19–21]. These local special functions, called *enrichments* are "pasted" using a partition of unity (PU) method [22–25]. The GFEM/XFEM has been extensively applied to the interface problem, see [12,15,26–36] for instance. The enrichments of GFEM/XFEM for the interface problem are the absolute of level set function or the distance function (to the interface curve Γ), D. Directly enriching D in the GFEM/XFEM causes a so-called blending element errors, as reported in [30]. To resolve it, a corrected XFEM was proposed in [30] by introducing an enrichment RD, where R is a cutoff function. The corrected XFEM enriches more freedoms of degree, and its conditioning gets bad as the interface approaches boundaries of elements. Recently, a stable GFEM (SGFEM) was introduced in [19,37,38] to improve the conditioning of GFEM/XFEM. The SGFEM enriches

$$D - \mathcal{I}_h D \tag{1.1}$$

instead of D, where $\mathcal{I}_h D$ is the standard FE interpolant of D. The SGFEM for interface problems is proven to have the optimal convergence in [19,28], and the conditioning is of the same order as that of the FEM and does not deteriorate as the interfaces approach the boundaries of elements. The applications of SGFEM ideas to the interface problems, crack problem, and high order approximations are referred to [19,26,28,31,36,38–41].

This paper is aimed to improve the enrichment D and associated numerical integrations in GFEM/XFEM and SGFEM for the interface problem. On the one hand, evaluations of D and its gradient are needed when assembling stiffness matrices. These evaluations require algorithms of computational geometry and could be difficult as the interface is geometrically complex. On the other hand, the numerical integration associated with D has not been resolved efficiently for the GFEM/XFEM and SGFEM. A standard integration rule in the GFEM/XFEM is to decompose the elements into subelements based on the interface [4,42]. The finer subelements were used to enhance accuracy in [31,43]. Another approach is to map the Gauss integration points in a higher-order reference element into the subelements [30,44]. Numerical integration rules using zero-level sets of level set functions were developed to address the implicit interface in [45–47]. A strategy circumventing volume integrations on elements was proposed in a smooth XFEM [48]. To the best of our knowledge, the studies on the numerical integration of GFEM/XFEM for the interface problem are only concentrated on algorithm designing, and a rigorous theoretical analysis on the integration error has not been provided in the literature. In this study, we propose a modified version of D, $|\mathcal{I}_{\Gamma,h}\vec{D}|$, to replace D in (1.1), and the new enrichment for the SGFEM is the following:

$$|\mathcal{I}_{\Gamma,h}\vec{D}| - \mathcal{I}_h|\mathcal{I}_{\Gamma,h}\vec{D}|, \tag{1.2}$$

where $\vec{D}$ is a smooth function defined based on D in (4.1), and $\mathcal{I}_{\Gamma,h}$ is an interpolation operator, which equals to $\mathcal{I}_h$ on the elements not cut by Γ and is the (piecewise) linear interpolation on the elements intersecting Γ. In $\mathcal{I}_{\Gamma,h}\vec{D}$, only the evaluation of D at the nodes close to Γ is needed, and the evaluation of gradients of D is not needed. This reduces the computational expense greatly. We prove that the zero-level set of $\mathcal{I}_{\Gamma,h}\vec{D}$, denoted by Γ_h, can approximate Γ with a high accuracy. Since $\mathcal{I}_{\Gamma,h}\vec{D}$ is the (piecewise) linear functions, Γ_h is also (piecewise) linear on the elements cut by Γ. Based on Γ_h we develop a perturbed variational problem, and then the numerical integration rule is designed to integrate such a variational form exactly. We prove that the SGFEM solution computed from the proposed variational problem and numerical integration can still achieve the optimal energy convergence order $O(h)$. This is verified by numerical experiments. The scaled condition number of proposed SGFEM is also shown to have the same order as that of FEM.

The paper is organized as follows. The model problem is described in Section 2. The conventional GFEM/XFEM and SGFEM are reviewed in Section 3. The SGFEM with the improved enrichment is proposed in Section 4, and the optimal approximation error is proven based on a perturbed variational problem. In Section 5, we design a numerical integration rule and prove that the approximation error of proposed SGFEM with the numerical integration is also optimal. The numerical experiments and concluding remarks are presented in Sections 6 and 7, respectively.

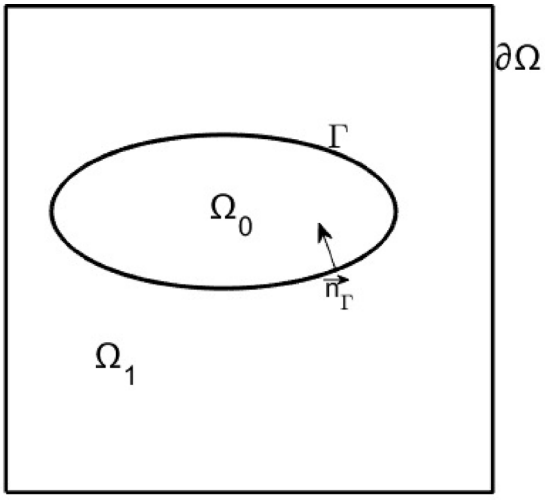

Fig. 1. The domains with a closed curved interface.

2. Model problem

For a domain Δ in $\mathbb{R}^2$, an integer m, and $1 \le q \le \infty$, we denote usual Sobolev spaces as $W^{m,q}(\Delta)$ with norm $\|\cdot\|_{W^{m,q}(\Delta)}$ and semi-norm $|\cdot|_{W^{m,q}(\Delta)}$. The space $W^{m,q}(\Delta)$ will be represented by $H^m(\Delta)$ for $q = 2$ and $L^q(\Delta)$ when $m = 0$, respectively.

We consider a bounded and simply connected domain $\Omega \subset \mathbb{R}^2$ with a piecewise smooth boundary $\partial\Omega$. Let Γ be an interface that divides Ω into two domains Ω_0 and Ω_1 such that $\overline{\Omega} = \overline{\Omega}_0 \cup \overline{\Omega}_1$, $\Omega_0 \cap \Omega_1 = \emptyset$, and $\Gamma = \overline{\Omega}_0 \cap \overline{\Omega}_1$. In this study, we consider that the interface Γ is closed and smooth, as shown in Fig. 1. For simplicity, we assume Γ is C^2 continuous.

A point in the Cartesian coordinate system of $\mathbb{R}^2$ is denoted as $P = (x, y)$. Let a be a positive, piecewise-constant function given by

$$a(P) = \begin{cases} a_0, & P \in \Omega_0, \\ a_1, & P \in \Omega_1, \end{cases} \tag{2.1}$$

where a_0 and a_1 are positive constants, $0 < \zeta_0 \le a_r \le \zeta_1 < \infty$, $r = 0, 1$, and $\zeta_0, \zeta_1 \in \mathbb{R}$. Clearly, a is discontinuous along the interface Γ.

We are interested in the solution u of the interface problem:

$$\begin{aligned} -\nabla \cdot (a\nabla u) &= f, \text{ in } \Omega, \\ u &= 0, \text{ on } \partial\Omega, \end{aligned} \tag{2.2}$$

subject to jump conditions on the interface Γ

$$[u]_\Gamma = 0, \quad \text{on } \Gamma, \tag{2.3}$$

$$\left[a\frac{\partial u}{\partial \vec{n}_\Gamma}\right]_\Gamma = 0, \quad \text{on } \Gamma, \tag{2.4}$$

where $\vec{n}_\Gamma$ denotes the unit vector normal to the interface Γ directed towards to Ω_0. The notation $[v]_\Gamma := v_1 - v_0$ defines the jump of a quantity v along the interface Γ, where $v_r := v|_{\overline{\Omega}_r}$, $r = 0, 1$.

The variational formulation of interface problem (2.2) is as follows:

$$\text{Find } u \in \mathcal{E}(\Omega) \text{ such that } B(u, v) = F(v), \ \forall v \in \mathcal{E}(\Omega), \tag{2.5}$$

where

$$B(u, v) = \int_\Omega a\nabla u \cdot \nabla v \, dP, \quad F(v) = \int_\Omega f v \, dP,$$

and $\mathcal{E}(\Omega)$ is an energy space given by

$$\mathcal{E}(\Omega) := \{v \in H_0^1(\Omega) : \|v\|^2_{\mathcal{E}(\Omega)} := B(v, v) < \infty \text{ and } [v]_\Gamma = 0 \text{ on } \Gamma\}.$$

Let $\mathbb{S}_h \subset \mathcal{E}(\Omega)$ is a finite dimensional subspace. Based on $\mathbb{S}_h$, the variational problem (2.5) is discretized as

$$\text{Find } u \in \mathbb{S}_h \text{ such that } B(u_h, v_h) = F(v_h), \ \forall v_h \in \mathbb{S}_h. \tag{2.6}$$

Using the standard Cea's lemma and the boundedness of a we have

$$\|u-u_h\|_{\mathcal{E}(\Omega)} \le \min_{v_h\in\mathbb{S}_h} \|u-v_h\|_{\mathcal{E}(\Omega)} \le \zeta_1 \min_{v_h\in\mathbb{S}_h} \|u-v_h\|_{H^1(\Omega)}. \tag{2.7}$$

This implies that an accurate approximation solution will be derived if a subspace $\mathbb{S}_h$ with good approximation property is designed.

The data f is given such that the solution $u \in \mathbb{M}_2$, where $\mathbb{M}_2$ is defined by

$$\mathbb{M}_2 := \{u : u|_{\Omega_r} \in H^2(\Omega_r),\ r=0,1 \ \text{ and } \|\partial^\alpha u\|_{L^\infty(\Gamma)} < \infty,\ |\alpha| \le 1\} \tag{2.8}$$

with a norm

$$\|u\|_{\mathbb{M}_2} = \|u_0\|_{H^2(\Omega_0)} + \|u_1\|_{H^2(\Omega_1)} + \sum_{|\alpha|\le 1} \|\partial^\alpha u\|_{L^\infty(\Gamma)},\ \forall u \in \mathbb{M}_2.$$

Remark 2.1. We present the model problem (2.2) using a homogeneous essential boundary condition for ease of exposition. The non-homogeneous essential boundary condition can be imposed directly by the FE part of the proposed SGFEM because we consider the closed interface (Γ does not intersect the boundary $\partial\Omega$), and the nodes on $\partial\Omega$ are not enriched by the extra functions. We consider the homogeneous interface condition (2.3) and (2.4), which gives a continuous solution u with discontinuous gradients. The various FEM or GFEM have been developed to address such an interface problem in the literature, such as [4,6,9,11,18,26,31,33,35,49], and references therein. The interface problem with the non-homogeneous interface condition can be transformed to the homogeneous case using approaches in [50,51] so that the idea in this paper can be applied. □

3. Conventional GFEM and SGFEM for interface problems

We begin with a quasi-uniform finite element mesh $\mathcal{T}_h = \{e_s\}_{s\in E_h}$ of the domain Ω with mesh size $0 < h < 1$, where E_h is the index set, and the finite elements e_s can be triangles or quadrilaterals. We note that the mesh $\mathcal{T}_h$ does not need to match the interface Γ. Let $\{P_i\}_{i\in I_h}$ be the set of finite element nodes associated with the mesh $\mathcal{T}_h$, where I_h is the index set of the nodes. For every $i \in I_h$, we consider the standard linear (bilinear for quadrilateral element) finite element hat function ϕ_i. The closure of support of ϕ_i is denoted by ω_i. Since the mesh is quasi-uniform, we have

$$\|\phi_i\|_{L^\infty(\Omega)} = \|\phi_i\|_{L^\infty(\omega_i)} \le 1, \qquad \|\nabla\phi_i\|_{L^\infty(\Omega)} = \|\nabla\phi_i\|_{L^\infty(\omega_i)} \le Ch^{-1}, \tag{3.1}$$

where the positive constant C is independent of h and i. It is well known that $\{\phi_i\}_{i\in I_h}$ form a partition of unity (PU) [22–24] subordinate to $\{\omega_i\}_{i\in I_h}$.

The standard FEM subspace to approximate the solution of (2.2) is given by

$$\mathbb{S}_h := \mathbb{S}_{FEM} = \text{span}\{\phi_i :\ i \in I_h\}. \tag{3.2}$$

For any continuous function v, we denote the FE interpolant of v by $\mathcal{I}_h v$:

$$\mathcal{I}_h v := \sum_{i\in I_h} v(P_i)\phi_i. \tag{3.3}$$

It is well known that the FEM (3.2) with the unfitted mesh cannot approximate the solution of the interface problem efficiently [6,31].

The generalized or extended FEM (GFEM/XFEM) [4,20] is a typical technique to approximate the non-smooth problem using the unfitted mesh. In a conventional GFEM/XFEM for the interface problems, the approximation subspace is

$$\mathbb{S}_h = \mathbb{S}_{FEM} \oplus \mathbb{S}_{ENR} \ \text{ and } \ \mathbb{S}_{ENR} = \text{span}\{\phi_i D :\ i \in I^\Gamma_{h,enr}\}, \tag{3.4}$$

where

$$D(P) = \text{dist}(P, \Gamma)$$

is a distance function (can be replaced with the absolute of a level set function) [4,27,31], and

$$I^\Gamma_{h,enr} = \{i \in I_h :\ P_i \in e_s \text{ where } \mathring{e}_s \cap \Gamma \ne \emptyset\}$$

is an index set, and the nodes in $I^\Gamma_{h,enr}$ are called the enriched nodes. It is easy to know that

$$\text{Card}(I^\Gamma_{h,enr}) := \text{cardinality of } I^\Gamma_{h,enr} = O(h^{-1}). \tag{3.5}$$

It was known early (e.g., [31]) that the GFEM/XFEM (3.4) only produce a sub-optimal convergence order $O(\sqrt{h})$ in energy norm due to effect of so-called blending elements [4,30]. The optimal convergence $O(h)$ can be attained by the corrected XFEM [4,30]. However, the corrected XFEM enriched more nodes, and its conditioning may "blow up" as the interface Γ is close to the boundaries of elements [34].

Recently, a stable GFEM (SGFEM) was introduced in [19,26,28,31,37–39] to improve the conditioning of GFEM/XFEM. The approximation subspace of the SGFEM for the interface problems is given by

$$\mathbb{S}_h = \mathbb{S}_{FEM} \oplus \mathbb{S}_{ENR} \text{ and } \mathbb{S}_{ENR} = \text{span}\{\phi_i(D - \mathcal{I}_h D) : i \in I^{\Gamma}_{h,enr}\}, \tag{3.6}$$

where $\mathcal{I}_h$ is the FE interpolation operator defined in (3.3). It was shown [26] that the SGFEM (3.6) for the interface problem (a) reaches the optimal convergence order $O(h)$ in energy norm, (b) has a scaled condition number (SCN, defined in (6.1)) of stiffness matrices $O(h^{-2})$ that is of same order as the FEM, and (c) is robust in that the convergence and SCN do not depend on the relative positions of the mesh and interfaces.

The convergence of SGFEM for the interface problem

The optimal convergence order of SGFEM (3.6) has been proven in [34,39]. Here, we present some key results in [34,39], based on which we will prove the optimal convergence of improved SGFEM in this paper. Recall that

$$u_r := u\big|_{\overline{\Omega}_r}, \quad r = 0, 1.$$

We continuously extend u_0 and u_1 to the entire domain Ω to obtain functions $\tilde{u}_0$ and $\tilde{u}_1$ in $H^2(\Omega) \cap W^{1,\infty}(\Omega)$ such that

$$\tilde{u}_r = u_r \text{ on } \Omega_r \text{ and } \|\tilde{u}_r\|_{H^2(\Omega)} \le C\|u_r\|_{H^2(\Omega_r)}, \quad \|\tilde{u}_r\|_{W^{1,\infty}(\Omega)} \le C\|u_r\|_{W^{1,\infty}(\Omega_r)}, \quad r = 0, 1, \tag{3.7}$$

where C is a positive constant independent of h (see [52]).

Lemma 3.1. *For each enriched node P_i, $i \in I^{\Gamma}_{h,enr}$, there is a linear polynomial ξ_i and a constant $c_i = \frac{1}{2}\left[\frac{\partial \tilde{u}_0}{\partial \vec{n}_\Gamma}(Q_i) - \frac{\partial \tilde{u}_1}{\partial \vec{n}_\Gamma}(Q_i)\right]$, $Q_i \in \omega_i \cap \Gamma$ such that*

$$\|u - \xi_i - c_i D\|^2_{H^m(\omega_i)} \le Ch^{4-2m}(\|\tilde{u}_0\|^2_{H^2(\omega_i)} + \|\tilde{u}_1\|^2_{H^2(\omega_i)}) + Ch^{6-2m}\Big(\sum_{|\alpha|\le 1}\|\partial^\alpha u\|^2_{L^\infty(\Gamma)}\Big), \ m = 0, 1, \tag{3.8}$$

and

$$\|u - \xi_i - c_i D\|^2_{L^\infty(\omega_i)} \le Ch^{2}(\|\tilde{u}_0\|^2_{H^2(\omega_i)} + \|\tilde{u}_1\|^2_{H^2(\omega_i)}) + Ch^{4}\Big(\sum_{|\alpha|\le 1}\|\partial^\alpha u\|^2_{L^\infty(\Gamma)}\Big). \tag{3.9}$$

The proof of Lemma 3.1 is referred to [53].

Theorem 3.2. *Suppose that $u \in \mathbb{M}_2$ is the solution of the interface problem (2.2)–(2.4), and u^h_{SG} is the SGFEM solution of variational problem (2.6) based on the finite-dimensional subspace $\mathbb{S}_h$ (3.6), then there exists $C > 0$ independent of h such that*

$$\|u - u^h_{SG}\|_{\mathcal{E}(\Omega)} \le Ch\|u\|_{\mathbb{M}_2}. \tag{3.10}$$

Proof. Using the results (3.8) and (3.9) in the proof of Theorem 4.4 in [34] and repeating the arguments in the proof of Theorem 4.4 in [34], we have that there is $v_{SG} \in \mathbb{S}_h$ (3.6) and a constant C that is independent of h such that

$$\|u - v_{SG}\| \le Ch\|u\|_{\mathbb{M}_2}. \tag{3.11}$$

(3.10) is obtained according to (3.11) and (2.7). □

4. An improved SGFEM and its theoretical analysis

In this section we design an improve enrichment for the SGFEM to reduce the computational complexity of evaluating D and its gradients. For this end, we define

$$\vec{D}(P) = \begin{cases} D(P), & P \in \Omega_0, \\ -D(P), & P \in \Omega_1. \end{cases} \tag{4.1}$$

Since we assume that the interface is smooth (C^2 continuous), $\vec{D}$ is smooth in that $\vec{D} \in W^{2,\infty}(\Omega)$. We next define an interpolant of $\vec{D}$. Let

$$E^{\Gamma}_h = \{s \in E_h : \mathring{e}_s \cap \Gamma \ne \emptyset\}, \tag{4.2}$$

i.e., E^{Γ}_h is the index set of elements intersecting Γ. If the initial mesh $\mathcal{T}_h$ is quadrilateral, we divide each e_s, $s \in E^{\Gamma}_h$ into two triangles through its diagonal, and all such triangles are indexed by $E^{\Gamma}_{h,T}$, see Fig. 2 one-three. If $\mathcal{T}_h$ is triangular, we also denote the index set of all triangular elements that intersect Γ by $E^{\Gamma}_{h,T}$, see Fig. 2 four-five. In this situation, it is clear that $E^{\Gamma}_{h,T} = E^{\Gamma}_h$, see Fig. 2 four-five. Therefore, the elements in $E^{\Gamma}_{h,T}$ are triangular for both the quadrilateral and triangular meshes, and a triangle in $E^{\Gamma}_{h,T}$ is denoted by $e^{\Gamma}_{s,T}$. We will explain later why the triangles in $E^{\Gamma}_{h,T}$ are used for the quadrilateral mesh. An interpolant of $\vec{D}$ based on $E^{\Gamma}_{h,T}$, denoted by $\mathcal{I}_{\Gamma,h}\vec{D}$, is defined as follows:

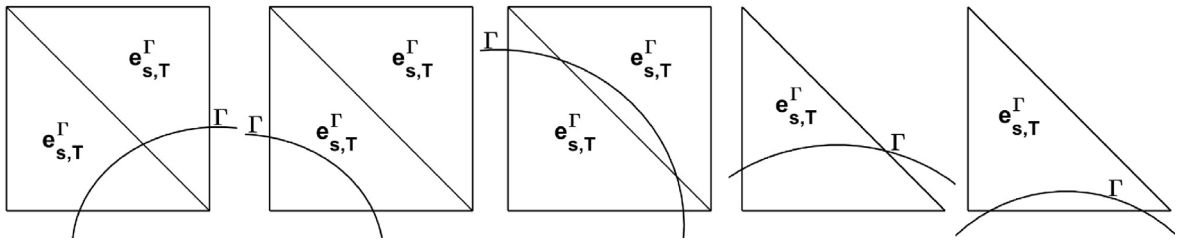

Fig. 2. The elements cut by Γ. One-three: quadrilateral elements; four-five: triangular elements. A quadrilateral element is divided into two triangles through its diagonal. All triangles in these figures are denoted by $e^{\Gamma}_{s,T}$, $s \in E^{\Gamma}_{h,T}$.

- for the triangular mesh, $\mathcal{I}_{\Gamma,h}\vec{D} = \mathcal{I}_h\vec{D}$, i.e., the standard FE interpolant used to define the SGFEM (3.6);
- for the quadrilateral mesh, for any $s \notin E^{\Gamma}_{h}$, $\mathcal{I}_{\Gamma,h}\vec{D}|_{e_s} = \mathcal{I}_h\vec{D}|_{e_s}$, which is the standard bilinear interpolant based the quadrilateral elements; for $s \in E^{\Gamma}_{h,T}$, $\mathcal{I}_{\Gamma,h}\vec{D}|_{e^{\Gamma}_{s,T}}$ is the standard linear interpolant based on the triangle $e^{\Gamma}_{s,T}$.

Therefore, $\mathcal{I}_{\Gamma,h}\vec{D}$ is a mixed interpolant for the quadrilateral mesh. For both the triangular and quadrilateral meshes we have

$$\mathcal{I}_{\Gamma,h}\vec{D}|_{e_s} = \mathcal{I}_h\vec{D}|_{e_s}, \forall\ s \notin E^{\Gamma}_{h}. \tag{4.3}$$

The following interpolation error holds according to the standard interpolation theory for both the triangular and quadrilateral meshes:

$$\|\vec{D} - \mathcal{I}_{\Gamma,h}\vec{D}\|_{W^{m,\infty}(\Omega)} \le Ch^{2-m}|\vec{D}|_{W^{2,\infty}(\Omega)} \le Ch^{2-m},\ m = 1, 2. \tag{4.4}$$

The approximation subspace of an improved SGFEM for the interface problems is given by

$$\mathbb{S}_h = \mathbb{S}_{FEM} \oplus \mathbb{S}_{ENR} \text{ and } \mathbb{S}_{ENR} = \text{span}\{\phi_i\left(|\mathcal{I}_{\Gamma,h}\vec{D}| - \mathcal{I}_h\left(|\mathcal{I}_{\Gamma,h}\vec{D}|\right)\right) :\ i \in I^{\Gamma}_{h,enr}\}. \tag{4.5}$$

It is noted by comparing (4.5) and (3.6) that only the distance function D is replaced by $|\mathcal{I}_{\Gamma,h}\vec{D}|$ in (3.6). First, in (4.5) $|\mathcal{I}_{\Gamma,h}\vec{D}| - \mathcal{I}_h\left(|\mathcal{I}_{\Gamma,h}\vec{D}|\right) = 0$ on the elements e_s that do not intersect Γ ($s \notin E^{\Gamma}_{h}$) according to (4.3). Second, in (4.5) only the values of D at the nodes in $I^{\Gamma}_{h,enr}$ are needed, and the derivatives of D are not needed for integrating global stiffness matrices. Therefore, the evaluations of D and its gradients in (3.6) are reduced greatly.

We next analyze the optimal approximation error of improved SGFEM (4.5).

Lemma 4.1. *For each enriched node P_i, $i \in I^{\Gamma}_{h,enr}$, there is a linear polynomial ξ_i and a constant $c_i = \frac{1}{2}\left[\frac{\partial\tilde{u}_0}{\partial\vec{n}_\Gamma}(Q_i) - \frac{\partial\tilde{u}_1}{\partial\vec{n}_\Gamma}(Q_i)\right]$, $Q_i \in \omega_i \cap \Gamma$ (the same as that in Lemma 3.1) such that*

$$\|u - \xi_i - c_i|\mathcal{I}_{\Gamma,h}\vec{D}|\|^2_{H^m(\omega_i)} \le Ch^{4-2m}(\|\tilde{u}_0\|^2_{H^2(\omega_i)} + \|\tilde{u}_1\|^2_{H^2(\omega_i)}) + Ch^{6-2m}\Big(\sum_{|\alpha|\le 1}\|\partial^\alpha u\|^2_{L^\infty(\Gamma)}\Big),\ \ m = 0, 1, \tag{4.6}$$

and

$$\|u - \xi_i - c_i|\mathcal{I}_{\Gamma,h}\vec{D}|\|^2_{L^\infty(\omega_i)} \le Ch^{2}(\|\tilde{u}_0\|^2_{H^2(\omega_i)} + \|\tilde{u}_1\|^2_{H^2(\omega_i)}) + Ch^{4}\Big(\sum_{|\alpha|\le 1}\|\partial^\alpha u\|^2_{L^\infty(\Gamma)}\Big). \tag{4.7}$$

Proof. Noting that for $m = 0, 1$,

$$\begin{aligned}||D - |\mathcal{I}_{\Gamma,h}\vec{D}|||_{W^{m,\infty}(\omega_i)} &= |||\vec{D}| - |\mathcal{I}_{\Gamma,h}\vec{D}|||_{W^{m,\infty}(\omega_i)}\\ &\le |||\vec{D} - \mathcal{I}_{\Gamma,h}\vec{D}|||_{W^{m,\infty}(\omega_i)} = ||\vec{D} - \mathcal{I}_{\Gamma,h}\vec{D}||_{W^{m,\infty}(\omega_i)} \le Ch^{2-m}|\vec{D}|_{W^{2,\infty}(\Omega)}.\end{aligned}$$

Therefore, using the estimate above and (3.8) yields that for $m = 0, 1$,

$$\begin{aligned}\|u - \xi_i - c_i|\mathcal{I}_{\Gamma,h}\vec{D}|\|^2_{H^m(\omega_i)} &\le 2\|u - \xi_i - c_iD\|^2_{H^m(\omega_i)} + 2c_i^2\|D - |\mathcal{I}_{\Gamma,h}\vec{D}|\|^2_{H^m(\omega_i)}\\ &\le Ch^{4-2m}(\|\tilde{u}_0\|^2_{H^2(\omega_i)} + \|\tilde{u}_1\|^2_{H^2(\omega_i)}) + Ch^{6-2m}\Big(\sum_{|\alpha|\le 1}\|\partial^\alpha u\|^2_{L^\infty(\Gamma)}\Big).\end{aligned}$$

The estimate (4.7) is obtained based on (3.9) in the similar way. □

Theorem 4.2. *Suppose that $u \in \mathbb{M}_2$ is the solution of the interface problem (2.2)–(2.4), and $u^{\Gamma,h}_{SG}$ is the solution of variational problem (2.6) based on the improved SGFEM finite-dimensional subspace $\mathbb{S}_h$ (4.5), then there exists $C > 0$ independent of h*

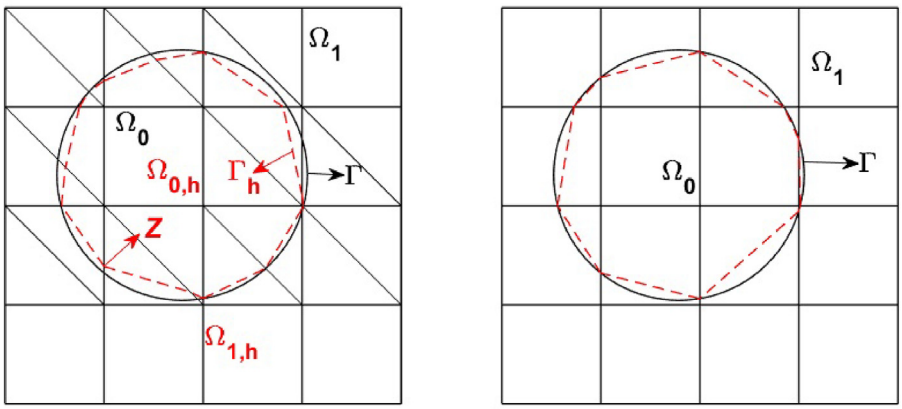

Fig. 3. The quadrilateral elements and a curved interface. Left: Γ_h is the zero-level set of $\mathcal{I}_{\Gamma,h}\vec{D}$. Γ_h is a polygonal line and is a straight line in a triangle in $\breve{E}^{\Gamma}_{h,T}$. The corners of Γ_h may not be on Γ, as shown by point "Z". Ω is divided into $\Omega_{l,h}, l = 0, 1$ by Γ_h. Right: another polygonal line to approximate Γ, which is derived by connecting cross points of Γ with boundaries of an element in a straight line, and all corners of this polygonal line are located on Γ.

such that

$$\|u - u_{SG}^{\Gamma,h}\|_{\mathcal{E}(\Omega)} \leq Ch\|u\|_{\mathbb{M}_2}. \tag{4.8}$$

Proof. Using the results (4.6) and (4.7) in the proof of Theorem 4.4 in [34] and repeating the arguments in the proof of Theorem 4.4 in [34], we have that there is $v_{SG} \in \mathbb{S}_h$ (4.5) and a constant C that is independent of h such that

$$\|u - v_{SG}\| \leq Ch\|u\|_{\mathbb{M}_2}. \tag{4.9}$$

(4.8) is obtained according to (4.9) and (2.7). □

Remark 4.1. Theorem 4.2 illustrates that the improved SGFEM (4.5) also yields the optimal order of convergence $O(h)$ for smooth interface problems. The proof is valid for both triangular and quadrilateral elements, where the mesh is fixed and unfitted, i.e., independent of the interface. We mention that the analysis in Theorem 4.2 is only based on the approximation property of $\mathbb{S}_h$ (4.5), which does not involve any interface coefficients. Thus, the SGFEM (4.5) addresses both the isotropic and anisotropic interface problem in a unified approach, and can also be applied to elasticity interface problems directly. □

5. Numerical integration and optimal approximation error

As reviewed in the Introduction part, various integration strategies for the GFEM/XFEM are developed in the literature, see [4,30,31,42,44–46,46,46–48] for instance. However, there is no mathematical analysis about effect of the numerical integration on the approximation order of GFEM/XFEM. In this section we design a numerical integration strategy for the improved SGFEM (4.5) and prove that the optimal approximation order $O(h)$ (in the energy norm) can be achieved based on such an integration rule.

We first present a piecewise linear approximation Γ_h to Γ, which is represented by the zero-level set of $\mathcal{I}_{\Gamma,h}\vec{D}$, i.e.,

$$\Gamma_h = \{P \in \Omega : \mathcal{I}_{\Gamma,h}\vec{D} = 0\},$$

see Fig. 3 Left for example. It is noted that for both the triangular and quadrilateral meshes, there are some triangles $e^{\Gamma}_{s,T}$ in $E^{\Gamma}_{h,T}$ do not contribute to the part of Γ_h (see Fig. 2 Left two and Left three (the top right-hand triangle) for a quadrilateral mesh and Fig. 2 five for a triangular element). The set of indices s in $E^{\Gamma}_{h,T}$ with $e^{\Gamma}_{s,T} \cap \Gamma_h \neq \emptyset$ are denoted by $\breve{E}^{\Gamma}_{h,T}$. It is easy to know that for each $s \in \breve{E}^{\Gamma}_{h,T}$, the part of Γ_h in $e^{\Gamma}_{s,T}$ is a straight line because $\mathcal{I}_{\Gamma,h}\vec{D}$ is a linear polynomial in $e^{\Gamma}_{s,T}$, see Fig. 4. The part (a straight line) of Γ_h in each $e^{\Gamma}_{s,T}$ is denoted by $\gamma^{\Gamma}_{s,T}$ (see Fig. 4), and we see that

$$\Gamma_h = \bigcup_{s \in \breve{E}^{\Gamma}_{h,T}} \gamma^{\Gamma}_{s,T}.$$

According to (4.4), we have that for any $P \in \Gamma_h$,

$$\text{dist}(P, \Gamma) = D(P) = |\vec{D}(P) - \mathcal{I}_{\Gamma,h}\vec{D}(P)| \leq Ch^2. \tag{5.1}$$

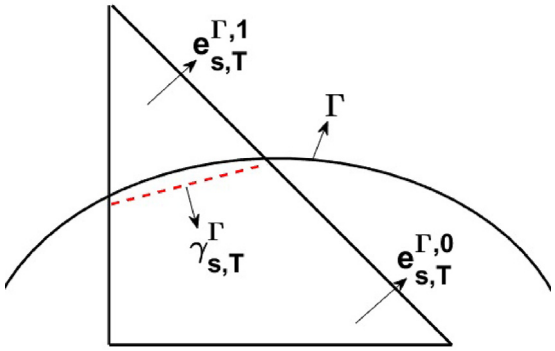

Fig. 4. A triangle $e^{\Gamma}_{s,T}, s \in \breve{E}^{\Gamma}_{h,T}$, is divided into two polygons $e^{\Gamma,0}_{s,T}$ and $e^{\Gamma,1}_{s,T}$ by $\gamma^{\Gamma}_{s,T}$, where $e^{\Gamma,1}_{s,T}$ is a triangle, and $e^{\Gamma,0}_{s,T}$ is a quadrilateral.

Namely, Γ_h approximates Γ with an order $O(h^2)$. We mention that the piecewise approximations Γ_h is different from the conventional approaches in the literature, where the cross points of Γ with boundaries of an element are connected in a straight line to approximate Γ [4,31,42], see Fig. 3 Right for example. The numerical integration in this paper is based on Γ_h.

The sub-domain enclosed by Γ_h is denoted by $\Omega_{0,h}$, and $\Omega_{1,h} = \Omega \setminus \Omega_{0,h}$ (see Fig. 3 Left), i.e., $\Omega_{0,h}$ and $\Omega_{1,h}$ have an interface Γ_h. Denote

$$L_h = (\overline{\Omega}_{0,h} \cap \overline{\Omega}_1) \cup (\overline{\Omega}_{1,h} \cap \overline{\Omega}_0), \tag{5.2}$$

which represents the union of mismatching part of $\overline{\Omega}_{0,h}$, $\overline{\Omega}_0$ and mismatching part of $\overline{\Omega}_{1,h}$, $\overline{\Omega}_1$. Using (5.1) produces

$$|L_h| \le Ch^2. \tag{5.3}$$

Every $e^{\Gamma}_{s,T}, s \in \breve{E}^{\Gamma}_{h,T}$ is cut into two parts by Γ_h, and the part in $\overline{\Omega}_{l,h}, l = 0, 1$ is denoted by $e^{\Gamma,l}_{s,T}$. It is obvious that $e^{\Gamma}_{s,T} = e^{\Gamma,0}_{s,T} \cup e^{\Gamma,1}_{s,T}$, see Fig. 4.

We note that $a(P)$ is not continuous in each $\Omega_{l,h}, l = 0, 1$. This will create the integration error. To this end, we define

$$a_h(P) = \begin{cases} a_0, & P \in \Omega_{0,h}, \\ a_1, & P \in \Omega_{1,h}, \end{cases} . \tag{5.4}$$

It is clear that a_h is a perturbation of a. We next define an approximation to f, f_h, as follows:

$$f_h(P) = \begin{cases} f(Q_s), & P \in e_s,\ s \in E_h \setminus E^{\Gamma}_h, Q_s \text{ is the center of } e_s, \\ f(T_s), & P \in e^{\Gamma}_{s,T},\ s \in E^{\Gamma}_{h,T} \setminus \breve{E}^{\Gamma}_{h,T}, T_s \text{ is the center of } e^{\Gamma}_{s,T}, \\ f(P^l_i), & P \in e^{\Gamma,l}_{s,T}, l = 0, 1,\ s \in \breve{E}^{\Gamma}_{h,T},\ P^l_i \text{ is a node of } e^{\Gamma}_{s,T} \text{ in } e^{\Gamma,l}_{s,T}, \end{cases} \tag{5.5}$$

see Fig. 5. It is clear that f_h is a piecewise constant function. We assume that $f \in C^1(\Omega_l), l = 0, 1$. Based on the definition of f_h we can obtain error estimates of f_h in what follows:

$$\|f - f_h\|_{L^\infty(\Omega \setminus L_h)} \le Ch|f|_{W^{1,\infty}(\Omega_0 \cup \Omega_1)} \tag{5.6}$$

and

$$\|f - f_h\|_{L^\infty(L_h)} \le 2\|f\|_{L^\infty(\Omega)}. \tag{5.7}$$

A perturbed variational formulation of (2.2) is developed as follows:

$$\text{Find } \tilde{u}^* \in \mathcal{E}(\Omega) \text{ such that } B^*_h(\tilde{u}^*, v) = F^*_h(v),\ \forall v \in \mathcal{E}(\Omega), \tag{5.8}$$

where

$$B^*_h(u, v) := \int_\Omega a_h \nabla u \cdot \nabla v \, dP, \quad F^*_h(v) := \int_\Omega f_h v \, dP.$$

The bilinear form $B^*_h(\cdot, \cdot)$ is a perturbation of $B(\cdot, \cdot)$, and it is easy to show that for any $v, w \in H^1(\Omega)$,

$$\frac{\zeta_0}{\zeta_1} B^*_h(v, v) \le B(v, v) \le \frac{\zeta_1}{\zeta_0} B^*_h(v, v) \tag{5.9}$$

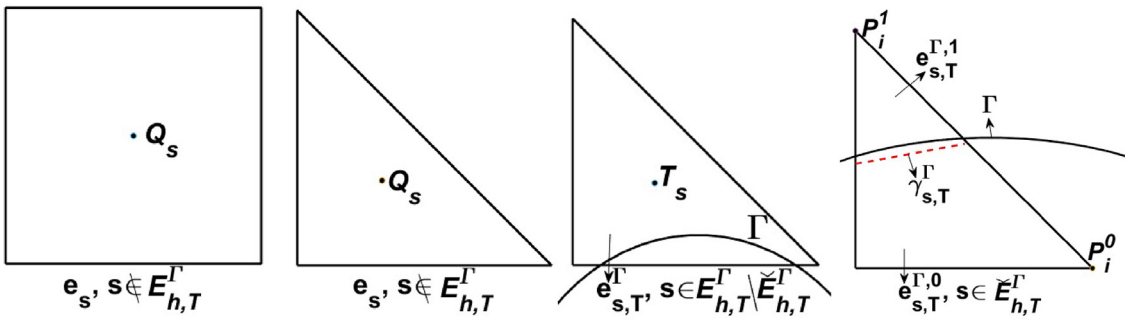

Fig. 5. The piecewise constant approximation to f on an element. Left one: a quadrilateral element not cut by Γ; left two: a triangular element not cut by Γ. Left three and four: triangles in $E^{\Gamma}_{h,T} \setminus \breve{E}^{\Gamma}_{h,T}$ and $\breve{E}^{\Gamma}_{h,T}$, respectively.

and

$$|B^*_h(v,w)| \le \sqrt{B^*_h(v,v)}\sqrt{B^*_h(w,w)} \le \frac{\zeta_1}{\zeta_0}\sqrt{B(v,v)}\sqrt{B(w,w)} = \frac{\zeta_1}{\zeta_0}\|v\|_{\mathcal{E}(\Omega)}\|w\|_{\mathcal{E}(\Omega)}. \tag{5.10}$$

Therefore, $B^*_h(\cdot,\cdot)$ is bounded and coercive in $\mathcal{E}(\Omega)$, and the variational problem (5.8) is uniquely solved.

Lemma 5.1. *Let u and $\tilde{u}^*$ be the solutions of the problems (2.5) and (5.8) respectively. Assume that $f \in C^1(\Omega_l), l = 0, 1$. Then there exists $C > 0$, independent of h, such that*

$$\|u - \tilde{u}^*\|_{\mathcal{E}(\Omega)} \le Ch(|u|_{W^{1,\infty}(\Omega)} + \|f\|_{W^{1,\infty}(\Omega_0\cup\Omega_1)}). \tag{5.11}$$

Proof. From (2.5) and (5.8) we have that for all $v \in \mathcal{E}(\Omega)$,

$$\begin{aligned}\int_\Omega (a - a_h)\nabla u \cdot \nabla v dP &= B(u,v) - B^*_h(u,v) = B(u,v) - B^*_h(\tilde{u}^*, v) - B^*_h(u - \tilde{u}^*, v)\\ &= F(v) - F^*_h(v) - B^*_h(u - \tilde{u}^*, v).\end{aligned}$$

Substituting $v = u - \tilde{u}^*$ in the equality above, and using Schwarz inequality and Poincarè inequality, we get

$$\begin{aligned}\frac{\zeta_0}{\zeta_1}\|u - \tilde{u}^*\|^2_{\mathcal{E}(\Omega)} &\le B^*_h(u - \tilde{u}^*, u - \tilde{u}^*)\\ &= \int_\Omega (a_h - a)\nabla u \cdot \nabla(u - \tilde{u}^*)dP + \int_\Omega (f - f_h)(u - \tilde{u}^*)dP\\ &\le \|(a_h - a)\nabla u\|_{L^2(\Omega)}|u - \tilde{u}^*|_{H^1(\Omega)} + C\|f - f_h\|_{L^2(\Omega)}|u - \tilde{u}^*|_{H^1(\Omega)}\\ &\le \frac{1}{\zeta_0}\|(a_h - a)\nabla u\|_{L^2(\Omega)}\|u - \tilde{u}^*\|_{\mathcal{E}(\Omega)} + C\frac{1}{\zeta_0}\|f - f_h\|_{L^2(\Omega)}\|u - \tilde{u}^*\|_{\mathcal{E}(\Omega)},\end{aligned}$$

where C is a coefficient in the Poincaré inequality, which is independent of h. Therefore,

$$\|u - \tilde{u}^*\|_{\mathcal{E}(\Omega)} \le \frac{\zeta_1}{\zeta_0^2}\left(\|(a_h - a)\nabla u\|_{L^2(\Omega)} + C\|f - f_h\|_{L^2(\Omega)}\right).$$

Finally we get (5.11) using the inequality above, (5.3), (5.6), (5.7), and following estimates:

$$\|(a_h - a)\nabla u\|^2_{L^2(\Omega)} = \int_{L_h}(a - a_h)^2|\nabla u|^2 dP \le C|L_h|(a_1 - a_2)^2|u|^2_{W^{1,\infty}(\Omega)} \le Ch^2(a_1 - a_0)^2|u|^2_{W^{1,\infty}(\Omega)}$$

and

$$\begin{aligned}\|f - f_h\|^2_{L^2(\Omega)} &= \int_{\Omega\setminus L_h}(f - f_h)^2 dP + \int_{L_h}(f - f_h)^2 dP \le Ch^2|f|^2_{W^{1,\infty}(\Omega_0\cup\Omega_1)}|\Omega \setminus L_h| + 2\|f\|^2_{L^\infty(\Omega)}|L_h|\\ &\le Ch^2|f|^2_{W^{1,\infty}(\Omega_0\cup\Omega_1)} + 2\|f\|^2_{L^\infty(\Omega)}Ch^2 \le Ch^2\|f\|^2_{W^{1,\infty}(\Omega_0\cup\Omega_1)}. \quad \square\end{aligned}$$

Solving the perturbed variational problem (5.8) based on the improved SGFEM subspace (4.5) gives the following discretized variational problem:

$$\text{Find } u^*_{SG} \in \mathcal{E}(\Omega) \text{ such that } B^*_h(u^*_{SG}, v_h) = F^*_h(v_h), \ \forall\ v_h \in \mathbb{S}_h \ (4.5). \tag{5.12}$$

Theorem 5.2. *Let u be the solutions of problem (2.5), and u_{SG}^* be the solution of (5.12) based on the improved SGFEM (4.5). Assume that $f \in C^1(\Omega_l)$, $l = 0, 1$. Then there exists $C > 0$, independent of h, such that*

$$\|u - u_{SG}^*\|_{\mathcal{E}(\Omega)} \leq Ch(|u|_{W^{1,\infty}(\Omega)} + \|f\|_{W^{1,\infty}(\Omega_0 \cup \Omega_1)}) + Ch\|u\|_{\mathbb{M}_2}. \tag{5.13}$$

Proof. According to (5.8) and (5.12) we have that for any $v_h \in \mathbb{S}_h$ (4.5),

$$B_h^*(\tilde{u}^* - u_{SG}^*, v_h) = 0.$$

Employing (5.9) and (5.10) we have

$$\begin{aligned}
\|\tilde{u}^* - u_{SG}^*\|_{\mathcal{E}(\Omega)}^2 &\leq \frac{\zeta_1}{\zeta_0} B_h^*(\tilde{u}^* - u_{SG}^*, \tilde{u}^* - u_{SG}^*) \\
&= \frac{\zeta_1}{\zeta_0} B_h^*(\tilde{u}^* - u_{SG}^*, \tilde{u}^* - v_h) \leq (\frac{\zeta_1}{\zeta_0})^2 B(\tilde{u}^* - u_{SG}^*, \tilde{u}^* - v_h) \\
&\leq (\frac{\zeta_1}{\zeta_0})^2 \|\tilde{u}^* - u_{SG}^*\|_{\mathcal{E}(\Omega)} \|\tilde{u}^* - v_h\|_{\mathcal{E}(\Omega)}
\end{aligned}$$

Therefore,

$$\|\tilde{u}^* - u_{SG}^*\|_{\mathcal{E}(\Omega)} \leq (\frac{\zeta_1}{\zeta_0})^2 \|\tilde{u}^* - v_h\|_{\mathcal{E}(\Omega)} \leq (\frac{\zeta_1}{\zeta_0})^2 \big(\|u - \tilde{u}^*\|_{\mathcal{E}(\Omega)} + \|u - v_h\|_{\mathcal{E}(\Omega)}\big), \ \forall\ v_h \in \mathbb{S}_h. \tag{5.14}$$

Then, taking $v_h = u_{SG}^{\Gamma,h}$ (in (4.8)) in (5.14) and using (5.14), (4.8), and (5.11), we have

$$\begin{aligned}
\|u - u_{SG}^*\|_{\mathcal{E}(\Omega)} &\leq \|u - \tilde{u}^*\|_{\mathcal{E}(\Omega)} + \|\tilde{u}^* - u_{SG}^*\|_{\mathcal{E}(\Omega)} \\
&\leq \big(1 + (\frac{\zeta_1}{\zeta_0})^2\big) \|u - \tilde{u}^*\|_{\mathcal{E}(\Omega)} + (\frac{\zeta_1}{\zeta_0})^2 \|u - u_{SG}^{\Gamma,h}\|_{\mathcal{E}(\Omega)} \\
&\leq Ch(|u|_{W^{1,\infty}(\Omega)} + \|f\|_{W^{1,\infty}(\Omega_0 \cup \Omega_1)}) + Ch\|u\|_{\mathbb{M}_2},
\end{aligned}$$

which is the desired result (5.13). □

Now we can describe the numerical integration rule based on the perturbed variational problem (5.12) and the improved SGFEM (4.5). Let $\xi_i, i \in I_h \cup I_{h,enr}^{\Gamma}$ be the basis of improve SGFEM subspace $\mathbb{S}_h$ (4.5), and then the entries of associated stiffness matrix and RHS are written as $B_h^*(\xi_j, \xi_i)$ and $F_h^*(\xi_i)$, $i, j \in I_h \cup I_{h,enr}^{\Gamma}$. The idea of numerical integration is to set the integration rules to exactly integrate these integration terms.

- For the triangular mesh, the integrands in $B_h^*(\xi_j, \xi_i)$ are constants on the elements e_s, $s \in E_h \backslash E_h^{\Gamma}$ and $e_{s,T}^{\Gamma}$, $s \in E_{h,T}^{\Gamma} \backslash \check{E}_{h,T}^{\Gamma}$, see Fig. 5 Left two and Left three. In these elements, the integrands in $F_h^*(\xi_i)$ are linear polynomials. Hence, we use the one-point Gauss rule (for the triangle) on these elements, which can exactly integrate these integrands. On $e_{s,T}^{\Gamma,l}, s \in \check{E}_{h,T}^{\Gamma}, l = 0, 1$, the integrands in $B_h^*(\xi_j, \xi_i)$ and $F_h^*(\xi_i)$ are the polynomials of degree two, and if $e_{s,T}^{\Gamma,l}$ is a triangle, the three-point Gauss rule is used; if $e_{s,T}^{\Gamma,l}$ is a quadrilateral, and $e_{s,T}^{\Gamma,l}$ is divided into two triangles, on each of which the three-point Gauss rule is used, see Fig. 5 Left four. Therefore, the integrations are exact on $e_{s,T}^{\Gamma,l}$ according to such an integration rule for both $B_h^*(\xi_j, \xi_i)$ and $F_h^*(\xi_i)$.
- For the quadrilateral mesh, the integrands in $B_h^*(\xi_j, \xi_i)$ are bi-quadratic polynomials on the elements $e_s, s \in E_h \setminus E_h^{\Gamma}$ (Fig. 5 Left one). In these elements (quadrilateral), the integrands in $F_h^*(\xi_i)$ are bi-linear polynomials. Hence, the two×two-Gauss rule and one-point Gauss rule on these elements are employed to exactly integrate the integrands associated with B_h^* and F_h^*, respectively. On the triangles $e_{s,T}^{\Gamma}, s \in E_{h,T}^{\Gamma} \setminus \check{E}_{h,T}^{\Gamma}$ and $e_{s,T}^{\Gamma,l}, s \in \check{E}_{h,T}^{\Gamma}, l = 0, 1$, the integrands $B_h^*(\xi_j, \xi_i)$ and $F_h^*(\xi_i)$ are the bi-fourth and bi-quadratic polynomials, respectively, see Fig. 5 Left three and Left four. Therefore, it is easy to set the Gauss rule on $e_{s,T}^{\Gamma}$ and $e_{s,T}^{\Gamma,l}$ ($e_{s,T}^{\Gamma,l}$ is divided into two triangles if it is a quadrilateral) to have the exact integrations in $B_h^*(\xi_j, \xi_i)$ and $F_h^*(\xi_i)$ on these elements.

According to the integration rule above, the integrations for B_h^* and F_h^* in (5.12) are exact, and thus the energy errors of SGFEM (5.12) under the proposed numerical integration rules are proven to be optimal ($O(h)$) in Theorem 5.2.

6. Numerical results

We consider the model problem (2.2) in a domain $\Omega = (0, 1)^2$, which is discretized by the uniform $n \times n$ square FE mesh with the mesh parameter $h = 1/n$. The FE shape functions we use are the bilinear functions associated with the square mesh. The model problem (2.2) with curved interfaces Γ are tested. We test two cases of coefficients: (i) $a_0 = 10$ and $a_1 = 1$, and (ii) $a_0 = 1$ and $a_1 = 100$. The manufactured exact solution u of (2.2) satisfying interface conditions (2.3)

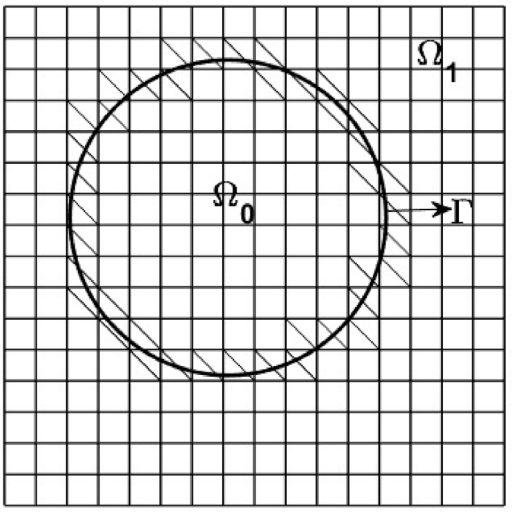

Fig. 6. A circular interface, and the mesh does not fit to the interface.

and (2.4) will be employed in the tests. The loading function f of (2.2) is calculated by using Eq. (2.2) and the manufactured solution u.

We will test the following methods for the numerical experiments below.

- FEM: standard bilinear FEM (3.2) based on the square mesh, where the mesh lines do not align with the interface curve,
- GFEM: GFEM (3.4) with enrichment D and enriched node set $I^{\Gamma}_{h,enr}$,
- SGFEM: SGFEM (3.6) with the distance function D and enriched node set $I^{\Gamma}_{h,enr}$,
- SGFEM$^{\text{imp}}$: the improved SGFEM (4.5) with the enrichment $|\mathcal{I}_{\Gamma,h}\vec{D}|$ and enriched node set $I^{\Gamma}_{h,enr}$.

We compute and compare the relative error in the energy norm (EE), i.e.,

$$EE = \frac{\|u - u_h\|_{\mathcal{E}(\Omega)}}{\|u\|_{\mathcal{E}(\Omega)}}$$

for the approximation solution u_h obtained from these methods, and the scaled condition number (SCN) of associated stiffness matrices $\mathbf{A}$. The SCN of $\mathbf{A}$ is defined by

$$\mathcal{K} := \kappa(\mathbf{DAD}), \tag{6.1}$$

where $\kappa(\cdot)$ is a condition number of a symmetric matrix, and $\mathbf{D}$ be a diagonal matrix with

$$\mathbf{D}_{ii} = \mathbf{A}_{ii}^{-1/2}.$$

We now present our numerical results in the following sub-sections.

6.1. An interface problem with a circular interface

We first consider an interface problem with a circular interface Γ; the equation of Γ is $(x - x_0)^2 + (y - y_0)^2 = r_0^2$, where $x_0 = \frac{1}{\sqrt{5}}, y_0 = \frac{1}{\sqrt{3}}, r_0 = \frac{1}{\sqrt{10}}$. In this case, we consider the manufactured solution of (2.2) as follows:

$$u = \begin{cases} \frac{2a_1}{(a_1-a_0)r_0^4} r^2 \cos(2\theta), & r < r_0 \ \ (\Omega_0), \\ \frac{a_1+a_0}{(a_1-a_0)r_0^4} r^2 \cos(2\theta) + r^{-2}\cos(2\theta), & r \geq r_0 \ \ (\Omega_1), \end{cases}$$

where (r, θ) is the polar coordinate at the center (x_0, y_0). It can be verified that u satisfies the interface condition (2.3) and (2.4), and is smooth on Ω_r, $r = 0, 1$. The mesh on the domain $[0, 1]\times[0, 1]$ is refined with $h^{-1} = n = 2^{j+1}$, $j = 3, 4, \ldots, 8$; see Fig. 6 for a display with $n = 16$. The EEs and SCNs with respect to h of the various methods mentioned above are presented in Fig. 7 for the different interface coefficients (10:1 and 1:100).

Fig. 7 clearly shows that the convergence order of the FEM, GFEM, SGFEM, and the improved SGFEM are $O(h^{0.5})$, $O(h^{0.5})$, $O(h)$, and $O(h)$, respectively, and their SCNs all increase with the order $O(h^{-2})$, which is the typical order of the SCN of FEM.

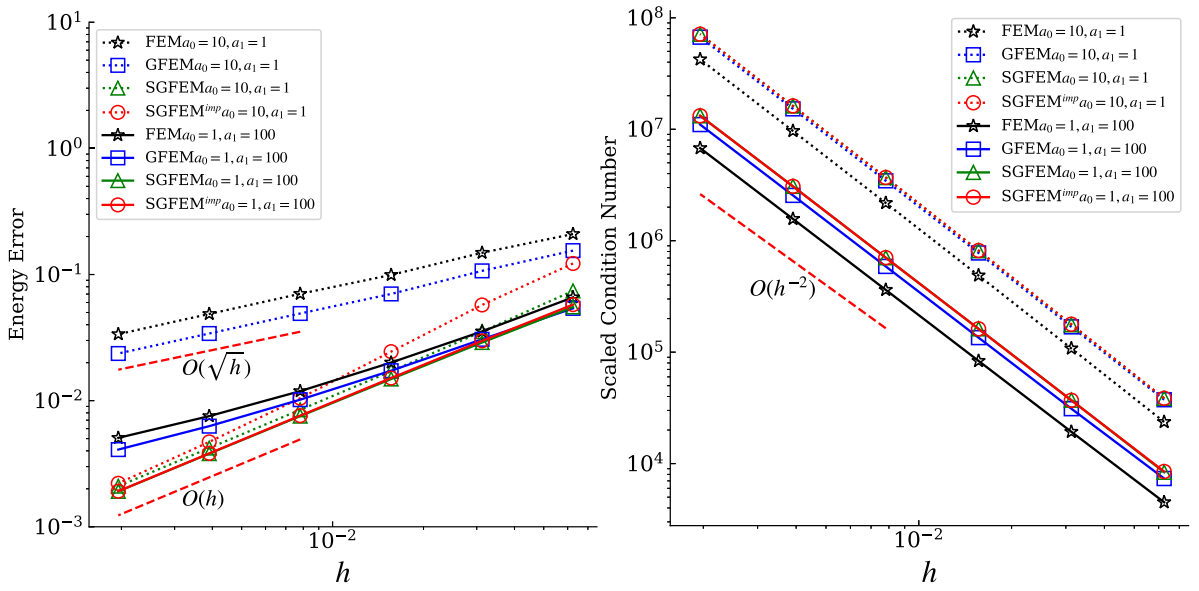

Fig. 7. The EEs and SCNs with respect to h of FEM, GFEM, SGFEM, the improved SGFEM for a circular interface problem with different interface coefficients. Left: EE. Right: SCN.

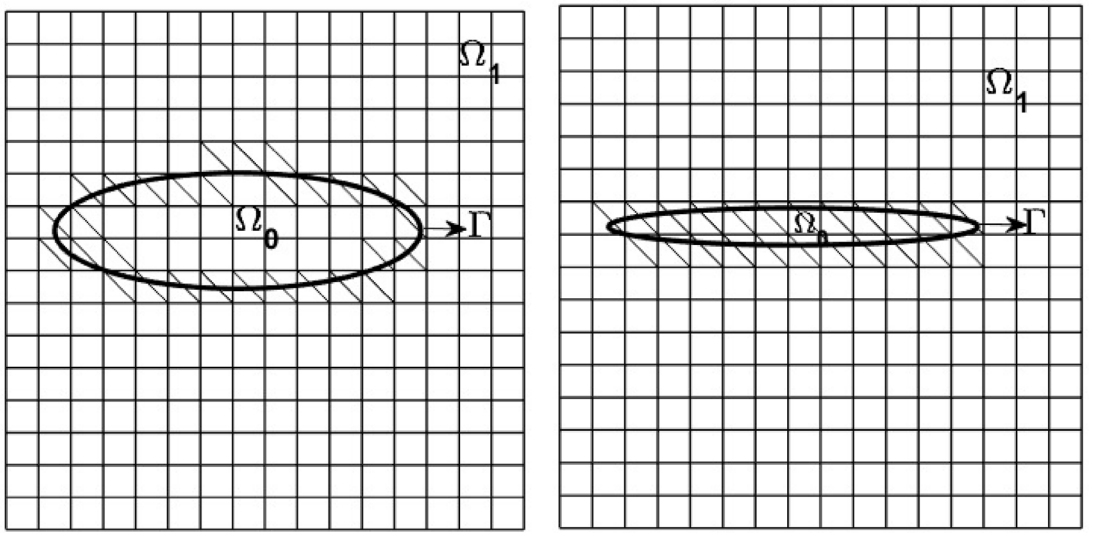

Fig. 8. Two ellipsoid interfaces, and the mesh does not fit to the interface.

6.2. Ellipsoid interfaces with different ratios of major and minor axes

We next test another curved interface problem containing ellipsoid interfaces Γ with different ratios of major and minor axes as follows:

$$\frac{(x-x_0)^2}{\alpha^2}+\frac{(y-y_0)^2}{\beta^2}=1,$$

where $x_0=\frac{1}{\sqrt{5}}, y_0=\frac{1}{\sqrt{3}}$. In this case the curvature of Γ is not a constant. We test the cases (a) $\alpha^2=\frac{1}{8}, \beta^2=\frac{1}{80}$ and (b) $\alpha^2=\frac{1}{8}, \beta^2=\frac{1}{800}$ to verify applicability of the improved SGFEM for varying curvatures, see Fig. 8. The manufactured

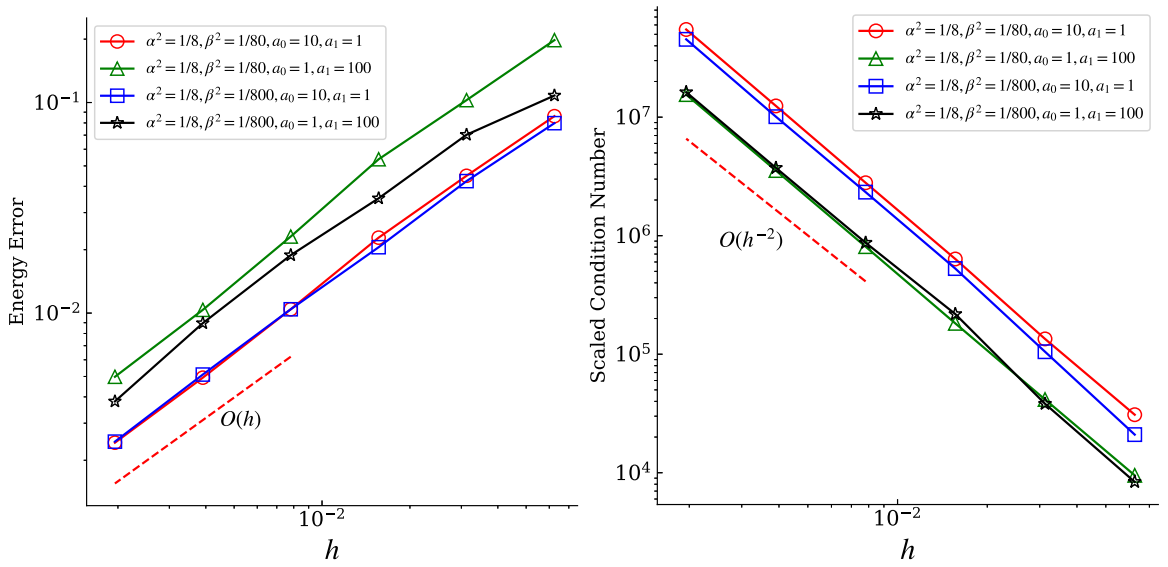

Fig. 9. The energy errors (Left) and the scaled condition numbers (Right) with respect to h of the improved SGFEM for ellipsoid interfaces with different ratios of major and minor axes and the interface coefficients.

solution of (2.2) we consider is the following:

$$u=\begin{cases} a_1(\frac{(x-x_0)^2}{\alpha^2}+\frac{(y-y_0)^2}{\beta^2}-1)e^{2x+y}, & \frac{(x-x_0)^2}{\alpha^2}+\frac{(y-y_0)^2}{\beta^2}<1\ \ (\Omega_0),\\ a_0(\frac{(x-x_0)^2}{\alpha^2}+\frac{(y-y_0)^2}{\beta^2}-1)e^{2x+y}, & \frac{(x-x_0)^2}{\alpha^2}+\frac{(y-y_0)^2}{\beta^2}\geq 1\ \ (\Omega_1), \end{cases}$$

It is easy to check that u satisfies the interface condition (2.3), and is smooth on $\Omega_r, r=0,1$. The mesh on the domain $[0,1]\times[0,1]$ is refined with $h^{-1}=n=2^{j+1}$, $j=3,4,\ldots,8$, see Fig. 8 for a display with $n=16$. The EEs and SCNs with respect to h of the improved SGFEM are presented in Fig. 9 for the different ratios of major and minor axes ((a) and (b)) and different coefficients (10:1 and 1:100).

It is clearly shown in Fig. 9 that in all the tested cases, the improved SGFEM converges with the optimal order $O(h)$, and its SCNs increase with the order $O(h^{-2})$, which is the same as that of FEM. The numerical experiments in this subsection demonstrate that the proposed SGFEM (4.5) also applies to the curved interface problems with varying curvatures.

7. Conclusions and comments

The SGFEM is a stable version of GFEM/XFEM, which (i) uses simple and unfitted meshes, (ii) reaches the optimal convergence order, and (iii) is stable and robust in the sense that conditioning is of the same order as that of FEM and does not get bad as interfaces approach boundaries of elements. This paper proposed an improved enrichment and a novel numerical integration rule for the SGFEM of interface problem. First, the complexity in evaluating the distance function and its gradients is reduced greatly. Especially, the values of gradients of the distance function are not needed. Second, it was proven that the SGFEM with the improved enrichment and the proposed integration rule can achieve the optimal convergence order for the interface problem. An extension of achievements in this paper to the situation of high order SGFEM is an interesting direction.

Data availability

Data will be made available on request.

References

[1] D.A. Edwards, H. Brenner, D.T. Wasan, Interfacial Transport Process and Rheology, Butterworths/Heinemann, London, 1991.
[2] Z. Li, K. Ito, The Immersed Interface Method: Numerical Solutions of PDEs Involving Interfaces and Irregular Domains, SIAM, 2006.
[3] C.S. Peskin, Numerical analysis of blood flow in heart, J. Comput. Phys. 25 (1977) 220–252.
[4] T.P. Fries, T. Belytschko, The extended/generalized finite element method: An overview of the method and its applications, Internat. J. Numer. Methods Engrg. 84 (2010) 253–304.
[5] I. Babuška, The finite element method for elliptic equations with discontinuous coefficients, Computing 5 (1970) 207–218.
[6] J.W. Barrett, C.M. Elliott, Fitted and unfitted finite-element methods for elliptic equations with smooth interfaces, IMA J. Numer. Anal. 7 (1987) 283–300.

[7] Z. Chen, J. Zou, Finite element methods and their convergence for elliptic and parabolic interface problems, J. Numer. Math. 79 (1998) 175–202.
[8] Z. Li, T. Lin, X. Wu, New cartesian grid methods for interface problems using the finite element formulation, Numer. Math. 96 (2003) 61–98.
[9] R. Guo, T. Lin, Y. Lin, Approximation capabilities of the immersed finite element spaces for elasticity interface problems, Numer. Methods Partial Differential Equations 35 (2019) 1243–1268.
[10] R. Guo, T. Lin, Y. Lin, Error estimates for a partially penalized immersed finite element method for elasticity interface problems, ESAIM Math. Model. Numer. Anal. 54 (2020) 1–24.
[11] A. Patel, S.K. Acharya, A.K. Pani, Stabilized Lagrange multiplier method for elliptic and parabolic interface problems, Appl. Numer. Math. 120 (2017) 287–304.
[12] A. Hansbo, P. Hansbo, An unfitted finite element method, Based on Nitsche's method, for elliptic interface problems, Comput. Methods Appl. Mech. Engrg. 191 (2002) 5537–5552.
[13] P. Hansbo, M.G. Larson, S. Zahedi, A cut finite element method for a Stokes interface problem, Appl. Numer. Math. 85 (2014) 90–114.
[14] P. Huang, H. Wu, Y. Xiao, An unfitted interface penalty finite element method for elliptic interface problems, Comput. Methods Appl. Mech. Engrg. 323 (2017) 439–460.
[15] C. Lehrenfeld, A. Reusken, Analysis of a Nitsche XFEM-DG discretization for a class of two-phase mass transport problems, SIAM J. Numer. Anal. 51 (2013) 958–983.
[16] Z. Cai, X. Ye, S. Zhang, Discontinuous Galerkin finite element methods for interface problems: A priori and a posteriori error estimations, SIAM J. Numer. Anal. 49 (2011) 1761–1787.
[17] R. Massjung, An unfitted discontinuous Galerkin method applied to elliptic interface problems, SIAM J. Numer. Anal. 50 (2012) 3134–3162.
[18] T. Lin, Y. Lin, X. Zhang, Partially penalized immersed finite element methods for elliptic interface problems, SIAM J. Numer. Anal. 53 (2015) 1121–1144.
[19] I. Babuška, U. Banerjee, Stable generalized finite element method(SGFEM), Comput. Methods Appl. Mech. Engrg. 201–204 (2011) 91–111.
[20] I. Babuška, U. Banerjee, J. Osborn, Survey of meshless and generalized finite element methods: a unified approach, Acta Numer. 12 (2003) 1–125.
[21] Y. Efendiev, T.Y. Hou, Multiscale Finite Element Methods: Theory and Applications, Springer, 2009.
[22] I. Babuška, J.M. Melenk, The partition of unity finite element method, Internat. J. Numer. Methods Engrg. 40 (1997) 727–758.
[23] C.A. Duarte, J.T. Oden, An h-p adaptive method using clouds, Comput. Methods Appl. Mech. Engrg. 139 (1996) 237–262.
[24] J.M. Melenk, I. Babuška, The partition of unity finite element method: Theory and application, Comput. Methods Appl. Mech. Engrg. 139 (1996) 289–314.
[25] Q. Zhang, C. Cui, Condensed generalized finite element method (CGFEM), Numer. Methods Partial Differential Equations 37 (2021) 1847–1868.
[26] I. Babuška, U. Banerjee, K. Kergrene, Strongly stable generalized finite element method: application to interface problems, Comput. Methods Appl. Mech. Engrg. 327 (2017) 58–92.
[27] N. Moës, M. Cloirec, P. Cartraud, J.F. Remacle, A computational approach to handle complex microstructure geometries, Comput. Methods Appl. Mech. Engrg. 192 (2003) 3163–3177.
[28] Q. Zhang, U. Banerjee, I. Babuška, Strongly stable generalized finite element method (SSGFEM) for a non-smooth interface problem, Comput. Methods Appl. Mech. Engrg. 344 (2019) 538–568.
[29] A.M. Aragon, C.A. Duarte, P.H. Geubelle, Generalized finite element enrichment functions for discontinuous gradient fields, Internat. J. Numer. Methods Engrg. 82 (2010) 242–268.
[30] K.W. Cheng, T.P. Fries, Higher-order XFEM for curved strong and weak discontinuities, Internat. J. Numer. Methods Engrg. 82 (2010) 564–590.
[31] K. Kergrene, I. Babuška, U. Banerjee, Stable generalized finite element method and associated iterative schemes: application to interface problems, Comput. Methods Appl. Mech. Engrg. 305 (2016) 1–36.
[32] M. Kirchhart, S. Gross, A. Reusken, Analysis of an XFEM discretization for Stokes interface problems, SIAM J. Sci. Comput. 38 (2016) A1019–A1043.
[33] P. Díez, R. Cottereau, S. Zlotnik, A stable extended FEM formulation for multi-phase problems enforcing the accuracy of the fluxes through Lagrange multipliers, Internat. J. Numer. Methods Engrg. 96 (2013) 303–322.
[34] P. Zhu, Q. Zhang, T. Liu, Stable generalized finite element method (SGFEM) for parabolic interface problems, J. Comput. Appl. Math. 367 (2020) 112475.
[35] J. Chessa, T. Belytschko, An extended finite element method for two-phase fluids, J. Appl. Mech. 70 (2003) 10–17.
[36] H. Sauerl, T.P. Fries, The stable XFEM for two-phase flows, Comput. & Fluids 87 (2013) 41–49.
[37] Q. Zhang, I. Babuska, U. Banerjee, High order stable generalized finite element methods, Numer. Math. 128 (2014) 1–29.
[38] V. Gupta, C.A. Duarte, I. Babuška, U. Banerjee, A stable and optimally convergent generalized FEM (SGFEM) for linear elastic fracture mechanics, Comput. Methods Appl. Mech. Engrg. 266 (2013) 23–39.
[39] Q. Zhang, I. Babuška, A stable generalized finite element method (SGFEM) of degree two for interface problems, Comput. Methods Appl. Mech. Engrg. 363 (2020) 112889.
[40] C. Cui, Q. Zhang, Stable generalized finite element methods (SGFEM) for elasticity crack problems, Internat. J. Numer. Methods Engrg. 121 (2020) 3066–3082.
[41] Q. Zhang, DOF-gathering stable generalized finite element methods (SGFEM) for crack problems, Numer. Methods Partial Differential Equations 36 (2020) 1209–1233.
[42] T. Belytschko, N. Moës, S. Usui, C. Parimi, Arbitrary discontinuities in finite elements, Internat. J. Numer. Methods Engrg. 50 (2001) 993–1013.
[43] K. Dréau, N. Chevaugeon, N. Moës, High order extended finite element method: influence of the geometrical representation, in: Proceedings of the 8th World Congress on Computational Mechanics (WCCM VIII), Venice, Italy, 2008.
[44] A. Legay, H. Wang, T. Belytschko, Strong and weak arbitrary discontinuities in spectral finite elements, Internat. J. Numer. Methods Engrg. 64 (2005) 991–1008.
[45] T.P. Fries, S. Omerović, Higher-order accurate integration of implicit geometries, Internat. J. Numer. Methods Engrg. 106 (2016) 323–371.
[46] K. Dréau, N. Chevaugeon, N. Moës, Studied X-FEM enrichment to handle material interfaces with higher order finite element, Comput. Methods Appl. Mech. Engrg. 199 (2010) 1922–1936.
[47] M. Kästner, S. Müller, J. Goldmann, C. Spieler, J. Brummund, V. Ulbricht, Higher-order extended FEM for weak discontinuities - level set representation, quadrature and application to magneto-mechanical problems, Internat. J. Numer. Methods Engrg. 93 (2013) 1403–1424.
[48] S. Bordas, T. Rabczuk, H. Hung, V. Nguyen, S. Natarajan, T. Bog, D. Quan, N. Hiep, Strain smoothing in FEM and XFEM, Comput. Struct. 88 (2010) 1419–1443.
[49] J. Ying, D. Xie, A new finite element and finite difference hybrid method for computing electrostatics of ionic solvated biomolecule, J. Comput. Phys. 298 (2015) 636–651.
[50] Z. Li, W. Wang, I.L. Chern, M. Lai, New formulations for interface problems in polar coordinates, SIAM J. Sci. Comput. 25 (2003) 224–245.
[51] L. Zhu, Z. Zhang, Z. Li, An immersed finite volume element method for 2D PDEs with discontinuous coefficients and non-homogeneuos jump conditions, Comput. Math. Appl. 70 (2015) 89–103.
[52] S.C. Brenner, L.R. Scott, The Mathematical Theory of Finite Element Methods, third ed., Springer, USA, 2008.
[53] Q. Zhang, C. Cui, U. Banerjee, I. Babuška, A condensed generalized finite element method (CGFEM) for interface problems, Comput. Methods Appl. Mech. Engrg. (2021) accepted.